RSC Advances

ROYAL SOCIETY OF CHEMISTRY

www.rsc.org/advances

RSC Advances

ARTICLE

Insight into the formation of a continuous sheath structure for PS phase in tri-continuous PVDF/PS/HDPE blends

Received 00th January 20xx,
Accepted 00th January 20xx

DOI: 10.1039/x0xx00000x

www.rsc.org/

Rui Dou, Shuanglin Li, Yan Shan, Bo Yin* and Mingbo Yang*

This work reports on the morphology development of ternary percolated co-continuous systems in PVDF/PS/HDPE blends in which PVDF and HDPE form two continuous networks, while the PS forms a continuous sheath structure at the PVDF/HDPE interface. By controlling the relative amounts of PVDF, PS and HDPE, continuity data based on gravimetric solvent extraction clearly demonstrate that a PS volume composition as low as 11% results in a very high level of continuity of about 80%. The evolution of PS phase continuity is further studied by changing the component ratio of HDPE and PS with PVDF phase concentration holds a constant value of 44 % volume fraction. Scanning electron microscope as well as optical microscope is used to clearly illustrate and identify the evolution of PS phase morphology. The results indicates that with PS phase concentration increase, the evolution of PS phase morphology in ternary blends experiences several distinguished stages: when PS concentration is less than 4 vol%, PS phase locates at PVDF and HDPE interface as dispersed droplets; when PS concentration increases to 7 vol%, PS phase forms incomplete interface between PVDF and HDPE; when PS concentration reaches 10 vol%, most of the PS has clearly and spontaneously structured itself at the PVDF/ HDPE interface forming a uniform layer. Additionally, the self-assemble behavior of PS droplets and the coalescence behavior of PS layer on the PVDF/HDPE interface are respectively investigated through online observation using optical microscope under quiescent annealing at 200 °C. The mechanism of phase morphology evolution under annealing indicates that the movement of phase interface and interfacial tension play a key role on the phase relax and equilibrium.

Introduction

The controlled formation of complex morphological multiphase materials is an important area of research in advanced materials science.[1-5] For binary immiscible polymer blends, two broad categories of morphology exist: the matrix/dispersed phase structure and the co-continuous morphology.[6] Recently, because multi-component polymer blends can demonstrate a wide variety of micro-structured morphologies with multiple interfaces present, more attention has been paid to the ternary polymer blends.[7-10]

For ternary polymer blends, complete wetting and partial wetting are two possible broad categories of morphological states. Hobbs et al.[10] employed a modified Harkins spreading theory (Equation (1)) to predict whether the morphology of a ternary blend is dominated by complete engulfing or by partial wetting.

$$\lambda_{BC} = \gamma_{AC} - \gamma_{AB} - \gamma_{BC} \quad (1a)$$

$$\lambda_{AC} = \gamma_{BC} - \gamma_{AB} - \gamma_{AC} \quad (1b)$$

$$\lambda_{AB} = \gamma_{CB} - \gamma_{AC} - \gamma_{AB} \quad (1c)$$

where the γ values are the interfacial tensions between the different phases. Each spreading coefficient gives the tendency of one phase to spread and form a continuous layer at the interface of the other two. If λ_{BC} is positive and the other two negative, then phase B forms a continuous phase between A and C and complete encapsulation is observed. In the case that all three spreading coefficients are negative, a partial wetting is observed in which none of the phases locate fully between the two others. For ABC ternary blends displaying complete wetting behavior with λ_{BC} is positive, four possible morphological hierarchies can be achieved and shown in Fig. 1. Fig. 1a, 1b and 1c illustrate the typical matrix/core-shell dispersed morphology and matrix/two separate dispersed phases morphology. Subsequently, increase the concentration of the core phase results in the coalescence of core phases which leads to the formation of a tri-continuous morphology (shown in Fig. 1d).

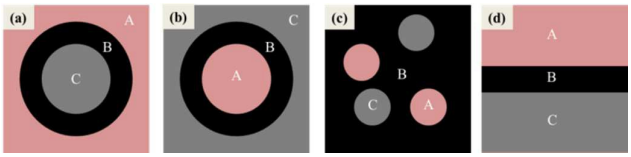

Fig.1 Equilibrium morphologies for a ABC ternary polymer system a) and b) matrix/core-shell dispersed phase morphology; c) matrix/two separate dispersed phase morphology; d) tri-continuous phase morphology describes complete wetting.

College of Polymer Science and Engineering, Sichuan University, State Key Laboratory of Polymer Materials Engineering, Chengdu, 610065 Sichuan, China.
Email: yangmb@scu.edu.cn & yinbo@scu.edu.cn

Generally speaking, continuous morphologies represent the special case where, in an A/B system, both components are fully continuous within the blend. Since this often occurs over a concentration range for binary polymer blends, this is also known as the region of dual phase continuity. By selectively controlling the interface,[11] composition,[12] processing temperature,[13] shear rate[14] and annealing time[15] of the blends, it is possible to control the pore size of the co-continuous network over 2-3 orders of magnitude. In an ABC system, the potential of tri-continuous structures is achieved by locating a phase with a specific characteristic at the interface of two other continuous phases. Because of the complex interface interaction of phases and the narrow window of phase continuous, the formation of this hierarchical multiphase continuous morphology is relatively difficult and only a limited works have been published.[7, 16-19] For example, Luzinov et al.[16] by employing Harkins equation, observed a tri-continuous structure in polystyrene/styrene–butadiene rubber/polyethylene (PS/SBR/PE) ternary blends with SBR as interfacial phase at a composition ratio of 30/25/45 wt%. They also found that with a constant content of SBR at 25 wt%, it was possible to maintain the tri-continuous structure whenever PS/PE composition ratio ranged from 40/60 to 60/40. Concerning with the control of tri-continuous structure in ternary blends, Favis et al studied a series of complete wetting polymer system such as PMMA/PS/HDPE,[17] PLA/PBAT/PBS,[18] and HDPE/PS/PCL,[19] and made significant contributions in the field of polymer morphology evolution. By employing 5 component continuous system of HDPE/PS/PMMA/PVDF/PANI blends, Favis et al.[20] found that conductive PANI percolation threshold can be reduced to below 5 vol%. Moreover, by employing the predication of interfacial tension and controlling the composition of phases, they developed a tri-continuous structure in which PS was situated at the interface of HDPE and PMMA and in this triple percolated system, a PS volume composition as low as 3% results in a PS phase continuity of about 70%, a very high level of continuity for such a small volume fraction of PS.[7] This instructive work has made the multiphase blends with tri-continuous structure as a candidate to design ultralow percolation threshold systems which are of particular interest in conductive applications.

In the case of the preparation of conductive ternary blends using tri-continuous structure, both interphase content and interphase layer thickness influence the percolation threshold. Therefore, the morphology control of tri-continuous structure in ternary blends should be clarified firstly. Ravati et al.[19] reported on the annealing of HDPE/PS/PCL ternary polymer blends with a tri-continuous structure. It was shown that the thickness of PS interfacial layer has increased from 2.3 μm before annealing to an average size of 112 μm after 30 min annealing.

However, the detailed morphological study of ternary blends demonstrating complete wetting structures is still insufficient, especially for the development from co-continuous in binary blends to tri-continuous morphology when the third interphase added. This paper therefore reports on the development of tri-continuous morphology in PVDF/PS/HDPE ternary blends. The morphology will be determined through a combination of electron and optical microscopy as well as through the estimation of continuity effects via selective solvent extraction/gravimetry of specific phases. The morphology evolution of ternary blends with low and high PS phase content was further investigated through an annealing process using optical microscopy equipped with heating stage.

Experimental

Materials

PVDF (type FR906) powder with an average molecular weight of 3.7×10^5 g/mol was obtained from Shanghai 3F New Materials Company (China). PS (type PG-33) pellets an average molecular weight of 1.2×10^5 g/mol were obtained from Taiwan Qimei Company. HDPE (type 2911) pellets with an average molecular weight of 1.7×10^5 g/mol were obtained from Fushun Petrochemical Company (China). The detail information of each component is notified in Table 1.

Table 1 Polymer characteristic.

	ρ (g/cm^3) at 25 ºC	ρ (g/cm^3) at 200 ºC	η_0 (Pa.s) at 0 s^{-1} at 200 ºC	η (Pa.s) at 50 s^{-1} at 200 ºC
PVDF	1.6	1.5	585.3	145.1
PS	1.05	0.95	4173.0	240.5
HDPE	0.93	0.85	377.2	187.6

Sample preparation

All polymers were dried in a vacuum oven for 24 h at 80°C before blending to minimize the effects of moisture. Various volume ratios of PS and HDPE pellets with 44 vol% PVDF powders were added simultaneously into a Haake torque mixer at 200 °C and 100 rpm for 8 min. The average shear rate was estimated to be γ=50 s^{-1} based on the type of mixer. Binary blends of HDPE/PVDF, PVDF/PS and HDPE/PS were prepared under the same procedure. After blending, the blends were quenched in cold water to freeze-in the morphology. Blends were annealed at 200 °C for 0, 5, 10, 15 and 20 min respectively using optical microscopy equipping with a heating stage.

Interfacial Tension Measurement

The interfacial tension for the pairs of polymers in this study was determined using the rheological behavior of their respective blend. The data were analyzed using Gramespasher and Meissner's analyses[21] following the procedures reported elsewhere.[22] The results concerning the interfacial tensions are listed in Table 2. These interfacial tension data are used to calculate the spreading coefficient:

$$\lambda_{AB} = \gamma_{BC} - \gamma_{AC} - \gamma_{BA} \quad (2)$$

where γ represents the interfacial tension for various polymer pairs and sub-indexes. A, B and C refer to each component. The spreading coefficient, λ_{AB}, is defined as the tendency of component (A) to encapsulate or spread onto component (B) in a matrix of component (C). A positive value of one of the spreading coefficients such as λ_{AB} demonstrates a complete

wetting morphology (two-phase contact) in which phase A spreads and forms a complete layer at the interface of phases B and C. Three negative spreading coefficients indicate a partial wetting behavior in which none of the three spreads at the interface of other phases and all three meet along a common line of three-phase contact. The calculated results are listed in Table 3. For ternary blends of PVDF/PS/HDPE, it is predicted that PS phase should be completely spread between PVDF and HDPE phases to form a complete wetting structure.

Table 2 Interfacial tension for polymer pairs at 200 °C.

Polymer pairs	Interfacial tension (mN/m)
PVDF/PS	4.7
PS/HDPE	3.4
HDPE/PVDF	11.9

Table 3 Spreading coefficients for the ternary PVDF/PS/HDPE systems at 200 °C.

	Spreading coefficient (mN/m)
λ(PS/HDPE)	3.8
λ(PVDF/PS)	-13.2
λ(HDPE/PVDF)	-10.6

Selective Solvent Extraction

Samples of 0.3−0.5 g were immersed in large volume of xylene and stirred gently at room temperature to selectively extract the PS component until the samples reached a constant weight. After extraction procedure the samples were dried in the vacuum oven at a temperature of 80 ºC for one day and the mass of the samples was determined. A gravimetric method was used to calculate the extent of continuity of the PS phase, using the simple equation:[6]

$$\%\text{continuity(A)} = \frac{m_{initial} - m_{final}}{m_{initial(A)}} \times 100 \quad (3)$$

in this equation, $m_{initial}$ is the initial mass of the sample, m_{final} is the final mass of the sample and $m_{initial(A)}$ is the initial mass of polymer A contained in the sample before selective extraction, calculated by its mass proportion based on the sample.

Morphology Characterization

For optical microscopy observations, 20μm thick specimens were prepared by a microtome. The morphologies of these thin sections were examined using Olympus BX51 polarizing optical microscopy (Olympus Co., Tokyo, Japan) under both bright field and crossed-polar conditions.. For SEM observations, the cryogenically fractured surface was directly coated with a thin layer of gold and observed at an accelerating voltage of 20.0 kV using a JEOL JSM-5900LV scanning electron microscopy (SEM, JEOL, Japan).

Quantitative analysis of the dispersed morphology was performed using image analysis of Image-Pro Plus 6. At least 300 dispersed domains were measured by manually tracing the phase boundaries to estimate number-average diameter (dn) for each sample. Corrections to the particles size were performed using Schwartz–Saltykov method.[23]

Results and discussion

Co-continuity window in PVDF/HDPE blends

In order to form a tri-continuous structure in PVDF/PS/HDPE ternary blends, the co-continuity window in PVDF/HDPE blends is firstly investigated. Fig. 2 presents the phase continuity of both components in PVDF/HDPE blends measured by selective solvent extraction as a function of volume fraction of PVDF. It can be seen that the HDPE component is continuous for the PVDF up to 60 vol%, whereas the PVDF component is continuous for the HDPE above 35 vol%. Therefore, the co-continuity window for PVDF/HDPE blends is PVDF of 35-60 vol %. Likewise, the inset polarized micrographs shows the dispersed PVDF phase type structure is converted to a continuous type structure through an increase in the PVDF composition. This conclusion was reached by considering the crystallization temperature of the materials as they cooled on the hot stage of the light microscope and then comparing that temperature to the crystallization temperatures of the neat materials. Pure PVDF and HDPE spherulites form at 146 ºC and 115 ºC. Such crystallization temperatures correspond to the DSC cooling run and crystalline peaks obtained for PVDF and HDPE (not shown here).

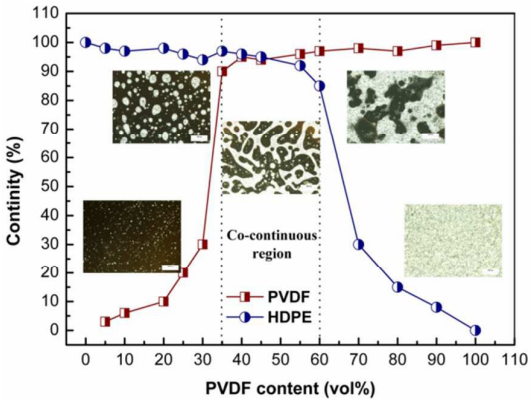

Fig. 2 Continuity of both components in PVDF/HDPE blends as a function of PVDF concentration, the inset polarized micrographs obtained at 140 ºC using POM (PVDF displays bright view while HDPE displays dark view).

Tri-continuous morphology in PVDF/PS/HDPE ternary blends

Ternary PVDF/PS/HDPE blends with tri-continuous structure were prepared based on the co-continuity region found for PVDF/HDPE binary blends. Moreover, Harkins spreading theory for the ternary PVDF/PS/HDPE blend shows a positive spreading coefficient of $\lambda_{PS/HDPE}$ with a value of 3.8 mN/m. It predicts complete wetting with the PS phase located at the interface of PVDF and HDPE. Experimental observations of the location of phases will be discussed in more detail below. Fig. 3 shows the phase morphology of PVDF/PS/HDPE ternary blends with a composition ratio of 44/20/36 vol%. SEM photos of PVDF/PS/HDPE blends in Fig. 3a displays a total continuous structure of different phase. In order to distinguish the phases, the PS is etched by xylene, uniform cracks pervade entirely throughout the sample (shown in Fig. 3b) can be

clearly seen, in contrast to Fig. 3a. In this case, gravimetric solvent extraction results reveal a 96 ± 2% continuity for PS. The EDS data of the other two areas in this sample are given. According to Fig. 3c, C and F atoms can be seen in one of the phases while the other phase only shows C atom. This demonstrates that the PVDF phase and HDPE phase can be accurately distinguished. Fig. 3d shows the polarized optical microscope (POM) image obtained at room temperature. It can be noted that the PVDF (bright white domains, corresponding to the crystalline structure) and HDPE phases (in dark yellow) appear as the main components and are separated by a thin PS layer (notice the black domains corresponding amorphous). Tri-continuous structure with the PS located at the interface between PVDF and HDPE is verified again.

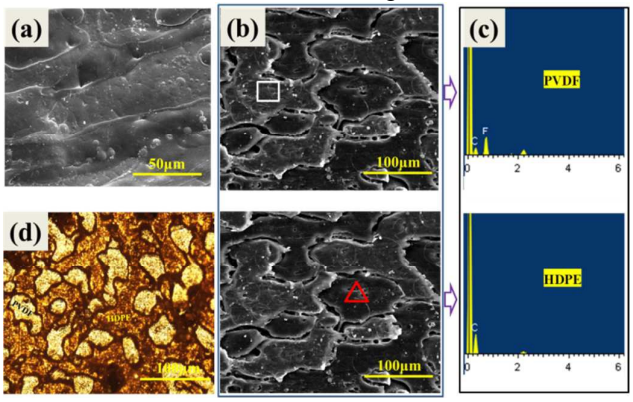

Fig. 3 The tri-continuous structure of PVDF/PS/HDPE (44/20/36 vol%) ternary blends (a) SEM micrograph of cryo-fractured surfaces, (b) SEM micrograph of cryo-fractured surfaces with PS etched by xylene, (c) EDS spectra of the areas marked by a white square and red triangle in b, (d) crystalline structures of samples under polarized optical microscopy after cooling down the temperature to crystalline temperature of phases.

Continuity curves of ternary PVDF/PS/HDPE, binary HDPE/PS and PVDF/PS blends

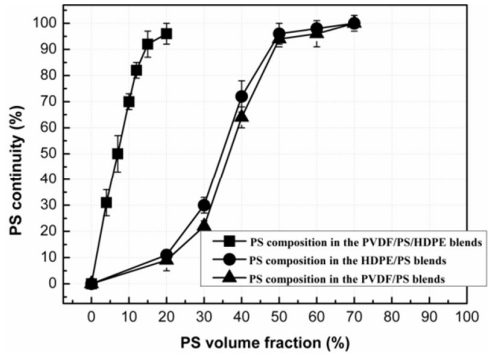

Fig. 4 Continuity of PS phase as a function of PS concentration in PVDF/PS/HDPE, HDPE/PS and PVDF/PS blends using the solvent dissolution technique (PVDF was hold a constant content of 44 vol% in PVDF/PS/HDPE blends).

The presence of a PS layer at the interface of the co-continuous PVDF/HDPE blends significantly reduces the PS volume fraction required for its percolation and continuity development as compared to classical binary HDPE/PS and PVDF/PS blends. Continuity data based on gravimetric solvent extraction clearly demonstrate this effect and are shown in Fig. 4. It can be seen that in this complete wetting triple phase system, a PS volume composition as low as 11 vol% results in a PS phase continuity of about 80%, a very high level of continuity for such a small volume fraction of PS. Moreover, the PS layer continuity increases with increasing PS volume content, reaching an apparent maximum value of approximately 95%.

The morphology of PVDF/PS/HDPE ternary blends after blending

SEM observation for the development of tri-continuous morphology with PS content increase

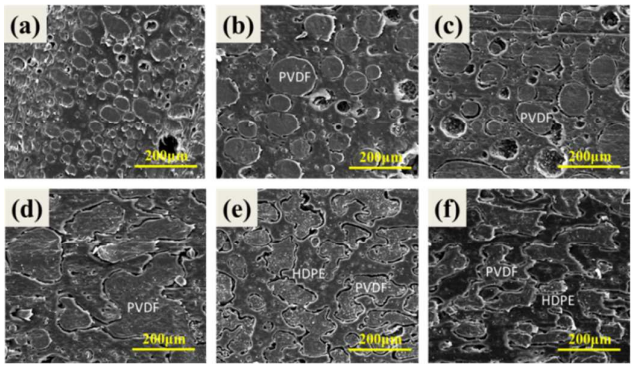

Fig. 5 SEM micrographs of morphology evolution of PVDF/PS/HDPE blends at various compositions, (a) 44/4/52 vol%; (b) 44/7/49 vol%; (c) 44/10/46 vol%; (d) 44/12/44 vol%; (e) 44/15/41 vol%, and (f) 44/20/36 vol%. (The PVDF is held constant at 44 vol% and PS phase is extracted by xylene in all samples).

Fig. 5 shows the morphology of the PVDF/PS/HDPE ternary blends of different volume fractions after extracting PS with xylene. As a global view from the images, the blends displays a matrix/dispersed phase morphology when PS content is less than 10 vol% (Fig. 5a, b and c) while the morphology changes into a tri-continuous morphology with PS content is more than 12 vol% (Fig. 5d, e and f). For tri-continuous morphology samples, it is clearly seen that the extracted PS phase forms a uniform crack, located at the interface of PVDF/HDPE that spreads entirely throughout the sample. However, for matrix/dispersed phase morphology samples, large PVDF droplets uniformly disperse in the HDPE matrix while PS phase forms small dispersed droplets around the PVDF particles due to lower PS concentration. More microstructure of PVDF/PS/HDPE blends with low content of PS is shown in Fig. 6. Fig. 6 exhibits the morphology for such a sample with 4 and 7 vol% PS from OM and SEM micrographs. For OM observations， although the phases can be recognized from the interfacial-angles, phase identification is also confirmed by the cooling temperature of the particular phase as it cools from the melt. This method requires that two important conditions be respected. Firstly, for a ternary blend, at least two components should be semi-crystalline with different crystallinity temperatures (shown in Fig. 2), and secondly, the crystallinity of the phases should not influence each other (confirmed in Fig.

3d). Fig 6a shows that at a 44/4/52 vol % composition, the resulting morphology consists of PS droplets located at the PVDF/HDPE interface with a fraction remaining in the HDPE phase. Their affinity for the HDPE side of the PVDF/HDPE interface is expected since the PS/HDPE has a interfacial tension of 3.2 mN/m which is lower than 4.9 mN/m of the PS/PVDF. With the PS content increases to 7 vol%, the coalescence of PS droplets into a layer that partly covers the PVDF phase (shown in Fig. 6b). Fig. 6c and d give the further SEM observation of this ternary blends with 4 vol% and 7 vol% PS respectively. In order to enhance the phase contrast of samples, PVDF and PS were successively extracted using DMF and xylene before SEM testing. Self-assembly of PS droplets into a perfectly close-packed droplet array at PVDF/HDPE interface can be clearly seen in Fig. 6c. Remarkably, when highly concentrated at the interface, the PS droplets coalesce into a partial layer at the interface (in Fig. 6d) and tend to form a uniform layer at higher PS content which has been proved by the above results (in Fig. 5d, e and f). This highly organized microstructure evolution is induced by the complete wetting of PVDF/HDPE interface by the PS phase.

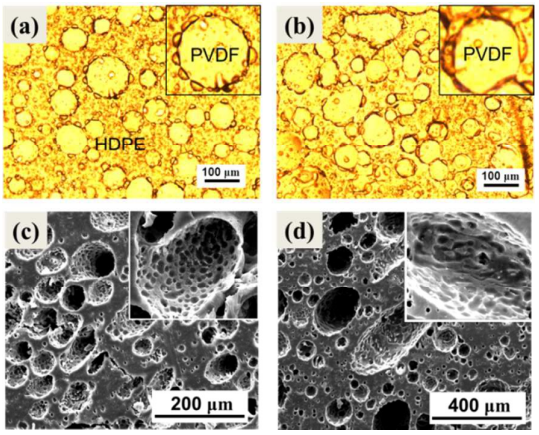

Fig. 6 Optical micrographs of PVDF/PS/HDPE at different composition ratios (a) 44/4/52 vol% and (b) 44/7/49 vol% ;SEM micrographs of PVDF/PS/HDPE at (c) 44/4/52 vol% and (d) 44/7/49 vol% composition ratios. (Optical micrographs were taken under 200 °C using optical mode, SEM photos were taken after PVDF and PS phase etched by DMF and xylene)

The mechanism of morphology evolution of PVDF/PS/HDPE blends during mixing

For all the ternary samples we studied, the concentration of the PVDF phase is held at 44 vol% and only the volume fraction of PS to HDPE changes. In all the cases, the volume fraction of PVDF based on the two major phases (PVDF and HDPE) changes from 46 % to 55 % which is still within their co-continuous window. However, the PVDF phase morphology changes from dispersed droplets to continuous region with PS content increasing. Moreover, the number average diameter of PVDF phase as a function of PS content in ternary blends is analyzed in Fig. 7. Compared with PVDF/HDPE binary blends, the introduction of PS phase lead to a decrease of PVDF phase size from 123 ± 10μm to 21 ± 0.7μm, subsequently the PVDF phase size increases with PS content increasing and reach a maximum value of 176 ± 12μm when PS content of 12 vol%. This PS content also presents the phase inversion of PVDF/PS/HDPE blends. Continue to increase PS content, the PVDF size decreases monotonously. How does one explain this morphology evolution during mixing? Two factors that can have a major impact on the evolution of the phase morphology in polymer blends are (1) the effect of interfacial tension on interfacial equilibration when PS introduces and (2) the variation of viscoelasticity when the components composition changes.

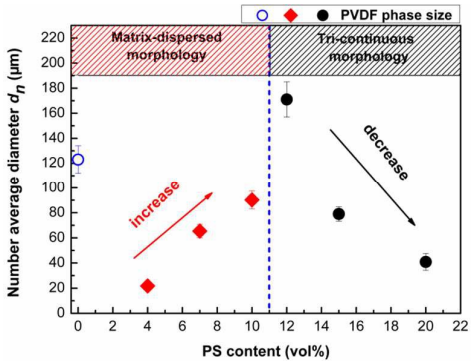

Fig. 7 PVDF phase number average diameter as a function of PS concentration in PVDF/PS/HDPE ternary blends (PVDF has a constant content of 44 vol%). The blue dash line represents the phase inversion according to Fig. 4 and 5.

According to the results listed in Table 2, PVDF/HDPE interfacial tension is 11.9 mN/m which is much larger than that of PVDF/PS and HDPE/PS. Also, PS has a much higher zero shear viscosity compared with PVDF and HDPE. The phenomenon that PVDF phase size decreases when PS introduces in PVDF/HDPE blends can be explained by means of capillary number Eq. 4:[24]

$$\mathrm{Ca} = \frac{\eta_m \alpha R}{\gamma} \quad (4)$$

where the capillary number Ca is a comparison between the viscous forces and the interfacial tension,[25, 26] R is the radius of the droplet, γ is the interfacial tension, η_m is the viscosity of the matrix, α is the shear rate during mixing. For our blends system, the calculated Ca increase about 3.7 times when PS phase adds which means an enhance tendency for phase break up, thus lead to the decrease of PVDF phase size. The subsequent increase of PVDF phase size when PS content lower than 12 vol% in ternary blends is mainly caused by concentration effect. It is well known that in a matrix/dispersed phase morphology blends, with the content of minor phase increasing, the size of dispersed droplets will enlarge due to coalescence of adjacent droplets.[27] In our ternary blends system, the morphology is consist of HDPE matrix, PVDF dispersed phase and PS dispersed phase when the content of PS is lower than 12 vol%. The volume fraction of PVDF based on HDPE and PVDF phases changes from 46 % to 50% with PS concentration increasing, thus resulting the increase of PVDF dispersed phase size.

The tri-continuous morphology with PS layer located in the interface of PVDF and HDPE is achieved when PS content reach to 12 vol% which is consistent with its thermodynamic equilibrium morphology. Therefore, the change of viscosity of the blends is mainly responsible for the size decrease of PVDF and it can be explained by the follow Eq. 5:[28]

$$\tau = \eta_m \alpha \quad (5)$$

Where τ is the shear stress, ηm is the viscosity of the matrix, α is the shear rate during mixing. On account of the preset condition of constant mixing parameters (mixing time, temperature and screw speed), a higher mixing energy input is provided for more viscous materials; high shear stresses are exerted by the highly viscous matrix phase leading to a better droplet break-up and less coalescence.[29] Also Taylor[30] observed that when the radius of the drop was great enough or when the rate of distortion was high, the drops break up. He developed Eq 6, which is an expression for determining the size of the largest drop that exists in a fluid undergoing distortion at any rate:

$$R = 2\gamma(\eta_d + \eta_m)/\alpha\eta_m\left(\frac{19}{4}\eta_d + 4\eta_m\right) \quad (6)$$

Where R is the radius of the droplet, γ is the interfacial tension, η_m and η_d is the viscosity of the matrix and dispersed phase respectively, α is the shear rate during mixing. For the PVDF/PS/HDPE ternary blends with a tri-continuous morphology, the γ between each two phases is constant, α is 50 s^{-1} for all the sample, only the viscosity of the system increases with PS phase increasing because of its higher viscosity (shown in Table 1), causing the decrease of PVDF phase size.

The self-assemble behavior of PS droplets on the PVDF/HDPE interface during melt annealing

For PVDF/PS/HDPE blends with low PS content, its morphology is consisted of PS droplets located at the HDPE/PVDF interface which is not complete wetting behaviors against the predication of interfacial tension. In order to better investigate the microstructure equilibrium behavior and better visualize the blends structure, quiescent annealing was carried out. Quiescent annealing allows the interfacial forces dominate and leads phase morphology to a thermodynamic steady state.[10, 31]

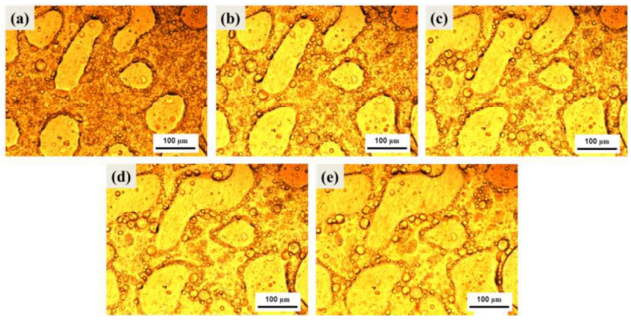

Fig. 8 Morphology evolution of PVDF/PS/HDPE 44/4/52 vol% blends as a function of annealing time (a) 0min, (b) 5 min, (c) 10min, (d) 15 min and (e) 20 min at 200 ºC by using OM.

The morphology evolution of PVDF/PS/HDPE with a composition ratio of 44/4/52 vol% can be noticed from Fig. 8. Before annealing for Fig. 8a, the first observed phenomenon is a partial and complete exclusion of PS from the PVDF/HDPE interface and HDPE region respectively. During annealing, the growth of the PVDF phase and PS droplet phase at the PVDF/HDPE interface is obviously seen from Fig. 8b-e. Additionally, after 20 min annealing, the number of PS droplets in HDPE regions largely decrease compared to the 0 min annealing case of Fig. 8a. The difference is striking and a divergence emerges for the PS droplet size during quiescent annealing as demonstrated in Fig. 9. It is clearly noticed that the size of PS at the interface is increasing with annealing while the size of PS in the HDPE regions is barely changed. Table 4 listed the calculated sizes of different phases. It is found that the average diameter increases from 11.2 ± 2.5 to 29 ± 2.4 μm for the PS droplets at the PVDF/HDPE interface after 20 min of annealing time, as compared to almost constant value of 4.8 μm for the PS droplets in HDPE region for the same annealing time. How do the large differences of two types of PS droplets morphology happened in PVDF/PS/HDPE blends under the same annealing condition?

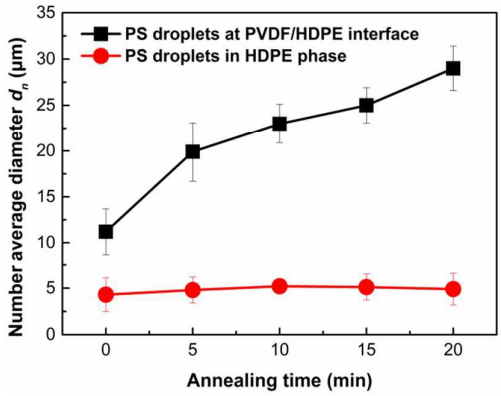

Fig. 9 Number average diameter d_n of the PS droplets at the interface and in the HDPE region for the PVDF/PS/HDPE 44/4/52 vol% blend as a function of annealing time.

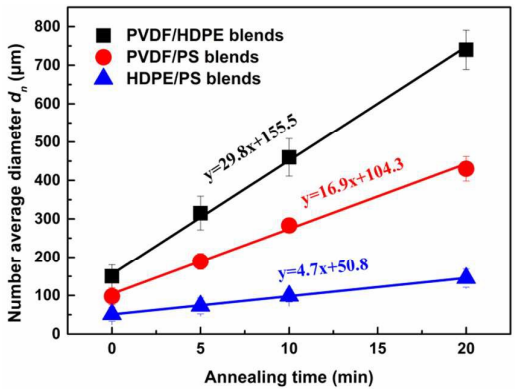

Fig. 10 Number average diameter d_n of the PVDF phase size in PVDF/HDPE and PS phase size in PVDF/PS and HDPE/PS blend as a function of annealing time (the lines represent the best linear fitting of each curve).

Table 4 Number average diameter d_n of different phases in the PVDF/PS/HDPE 44/4/52 vol% blend.

Annealing time (min)	d_n (PS at the interface, μm)	d_n (PS in the HDPE regions, μm)	d_n (PVDF phases, μm)
0	11.2 ± 2.5	4.3 ± 1.8	97.1 ± 10.6
5	19.9 ± 3.2	4.8 ± 1.4	103.4 ± 10.1
10	23.3 ± 2.1	5.2 ± 0.6	110.3 ± 9.8
15	25.1 ± 1.9	5.1 ± 1.4	117.7 ± 8.7
20	29.8 ± 24	4.9 ± 1.7	125.8 ± 11.2

In order to understand the change of PS droplet size at the PVDF/HDPE interface and HDPE regions during annealing, it is necessary to consider the factors that influence the phase relax and evolution such as viscoelastic,[10] inertial effects,[24] interfacial motion[31] and interfacial forces.[32] Actually the kinetics related to interfacial motion and the role of interfacial forces are the two key factors to control the evolution of phase morphology during quiescent annealing. The ability of interfacial motion for different polymer pairs is firstly investigated in each binary blend during quiescent annealing. And the phase coalescence rates can be as a simple standard to measure the ability of interfacial motion.[33-35] Therefore, the PVDF phase size in PVDF/HDPE and PS phase size in PVDF/PS or HDPE/PS were calculated and the results are shown in Fig. 10.

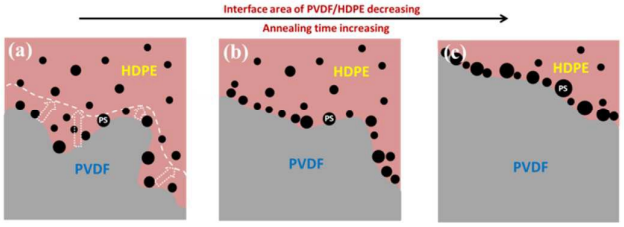

Fig. 11 Schematic map showing the morphology evolution of PVDF/PS/HDPE 44/4/52 vol% blends during annealing at 200 ºC. The gray region represents PVDF, the red region represents HDPE and the black droplets are PS. The white arrows in part (a) indicate the movement of PVDF/HDPE interface, (b) the PS droplets in HDPE phase are trapped on the PVDF/HDPE interface due to the movement of PVDF/HDPE interface and (c) the trapped PS droplets on the interface are force to contact and coalesce caused by the decrease of PVDF/HDPE interface.

Clearly, significant differences of coalescence rates are observed for different blends. Here we define a parameter K, which means the increment of phase size per unit time, to represent the coalescence rates. The linear fitting data reveal that K of PVDF/HDPE has the largest value of 29.8 compared to 16.9 for PVDF/PS and 4.7 for HDPE/PS blends. This results mean the ability of PVDF/HDPE interfacial motion>PVDF/PS > HDPE/PS. Therefore, for PVDF/PS/HDPE blends, during annealing, the fast coalescence rates of PVDF/HDPE domains cause the overall PVDF/HDPE interfacial area decreases, which has been demonstrated for many research.[34,36-38] This signifies a movement of the PVDF/HDPE interface, which can trap PS droplets located in the HDPE phase while moving, increasing the number of PS droplets at the PVDF/HDPE interface. Since the PS droplets are more thermodynamically stable when located at the PVDF/HDPE interface, more and more PS droplets will be trapped on the interface during annealing. Because of a higher interface area, this trapping effect is significant at initial annealing. With the decrease of PVDF/HDPE interface, the trapped PS droplets on the interface are force to contact and coalesce, thus resulting size increase of PS droplet. This morphology evolution is illustrated in Fig. 11. Moreover, because HDPE/PS has inferior ability of interfacial motion and combining the above analysis, this is why the size of PS droplets in HDPE regions barely increases during annealing (shown in Fig. 10).

The coalescence behavior of PS layer on the PVDF/HDPE interface during melt annealing

With the concentration of the PS phase increasing, the coalescence of PS phases on the PVDF/HDPE interface will lead to the formation of a tri-continuous morphology

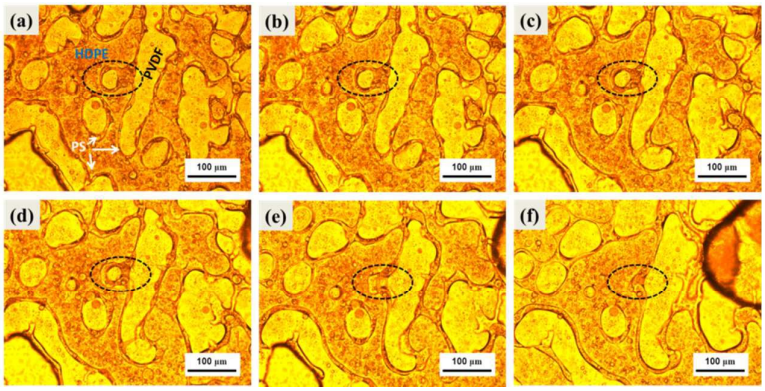

Fig. 12 Morphology evolution of PVDF/PS/HDPE 44/15/41 vol% blends as a function of annealing time (a) 0min, (b) 5 min, (c) 10min, (d) 15 min and (e) 20 min (f) 30 min at 200 ºC by using OM.

In this part, the coalescence behavior of the PS interfacial layer in ternary PVDF/PS/HDPE is studied during annealing. Fig. 12a illustrates the tri-continuous structure of the PVDF/PS/HDPE blend. It shows that most PS phase is formed a continuous layer to locate at the PVDF/HDPE interface. There are still some PS droplets embed in HDPE regions which caused by a lower interfacial tension of HDPE/PS than that of PVDF/PS. Also minority PVDF/PS core-shell dispersed droplets (shown by black circle in Fig. 12) can be found in HDPE regions. During annealing, these core-shell droplets are tended to trap by the large region phases because of the movement of phase interface, thus resulting the increase of phase size. Fig. 12f shows the sample after 30 min annealing and the thickness of PS layer has increased from 5.3 ± 0.8μm before annealing to 14.2 ± 1.2 μm after 30 min annealing.

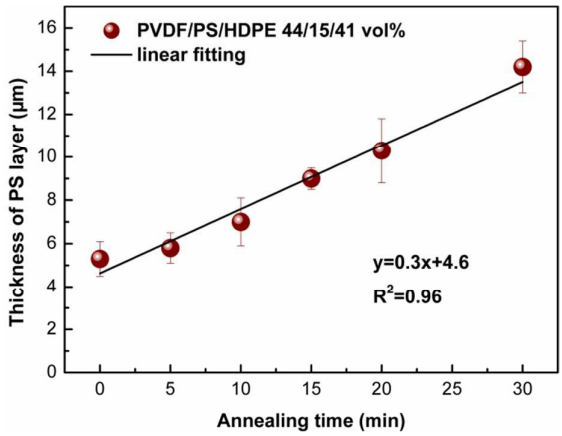

Fig. 13 The thickness of PS layer in PVDF/PS/HDPE 44/15/41 vol% blend as a function of annealing time.

Quantification of the thickness of PS layer as a function of annealing time is shown in Fig. 13. The growth rate for the thickness of the PS layer shows a clear linear relationship with annealing time with relative value of 0.3 μm/min. The quantitative linear growth of phase thickness with time for the interfacial layer in this tri-continuous ternary blend suggests a similar mechanism as with co-continuous binary blend systems.[39] Yuan et al.[16] proposed that the driving force for the coarsening process under static annealing is a result of capillary pressure and showed that the linear coarsening growth rate is dependent on the interfacial tension between phases, the viscosity ratio of the phases and the zero-shear viscosity of the matrix. The interfacial layer growth rate, however, in our tri-continuous system is significantly lower than the coarsening rates in the binary co-continuous case (shown in Fig. 10). The reason for the very low growth rate in the completely wet tri-continuous ternary case is due to the fact that the confinement effect of PS layer on the movement between PVDF and HDPE interface. The PS phase has a very large zero shear viscosity of 4173.0 Pa.s compared with 377.2 Pa.s for PVDF and 585.3 Pa.s for HDPE and the PS phase located at the PVDF/HDPE interface will tune the interfacial tension of phase interfaces which make a more stable thermodynamically structure.

Conclusions

In this work, the morphology development of PVDF/PS/HDPE ternary blends after melt mixing and during quiescent annealing is studied. The Harkins spreading theory indicates that PS phase is spread over the PVDF/HDPE interface formed a complete wetting structure. It has be found that PS phase can be form a continuous sheath structure at the PVDF/HDPE interface when its concentration reaches 11 vol%. With the PS concentration increasing, PS phase morphology in ternary blends experiences several distinguished stages: when PS concentration is less than 4 vol%, PS phase locates at PVDF and HDPE interface as dispersed droplets; when PS concentration increases to 7 vol%, PS phase forms incomplete interface between PVDF and HDPE; when PS concentration reaches 10 vol%, most of the PS has clearly and spontaneously structured itself at the HDPE/PMMA interface forming a uniform layer. The self-assemble behavior of PS droplets on the PVDF/HDPE interface during annealing is caused by interface trap effect induced by the decrease of interface area. This can be well understood from Harkins spreading theory and the coarsening of the PVDF/HDPE co-continuous structure. The interfacial coalescence of PS layer manifests that the thickness of PS layer has increased from 5.3 ± 0.8 μm before annealing to 14.2 ± 1.2 μm after 30 min annealing. The growth rate for the thickness of the PS layer shows a lower value of 0.3 μm/min which is cause by the confinement effect of PS layer on the movement between PVDF and HDPE interface.

Acknowledgements

The authors gratefully acknowledge the financial support from the National Natural Science Foundation of China (Contract No. 51273219, 51573106 and 5142106), the National Key Basic Research Program of China (973 Program, No. 2012CB025902), the Fundamental Research Funds for the Central Universities (No. 2013SCU04A03) and the Foundation of State Key Laboratory of Polymer Materials Engineering (Grant No. sklpme2014-3-12).

References

1 D. R. Paul, J. W. Barlow and H. Keskkula. Encyclopedia of polymer science and engineering. New York: Wiley; 1988.
2 R. A. Kudva, H. Keskkula and D. R. Paul, *Polymer*, 2000, **41**, 239-258.
3 B. Yin, L. P. Li, Y. Zhou, L. Gong, M. B. Yang and B. H. Xie, *Polymer*, 2013, **54**, 1938-1947.
4 T. Y. Zhao, C. Zhang, Z. J Du, H.Q Li and W. Zou, *RSC Advances*, 2015, **5**, 91516-91523.
5 B. D. Favis. In: D. R. Paul, C. B. Bucknall, editors. Polymer blends: formulation and performance, two-volume set, vol. 1. New York: John Wiley & Sons, Inc; 2000. p. 239.
6 J. Zhang, S. Ravati, N. Virgilio and B. D. Favis. *Macromolecules*, 2007, **40**, 8817.

7 R. Dou, C. Shen, B. Yin, M. B. Yang and B. H. Xie. *RSC Advances*, 2015, **5**, 14592-14602.
8 Z. Ke, D. Shi, J. H. Yin, R. Li and Y. W. Mai, *Macromolecules*, 2008, **41**, 7264-7267.
9 P. L. Corroller and B. D. Favis, *Polymer*, 2011, **52**, 3827-3834.
10 S. Y. Hobbs, M. E. J. Dekkers and V. H. Watkins. *Polymer*, 1988, **29**, 1598.
11 C. L. Zhang, L. F. Feng, J. Zhao, H. Huang, S. Hoppe and G. H. Hu, *Polymer,* 2008, **49**, 3462–3469.
12 N. Marin and B. D. Favis, *Polymer,* 2002, **43**, 4723-4731.
13 P. Sarazin and B. D. Favis, *Polymer,* 2005, **46**, 5966-5978.
14 K. Min, J. L. White and J. F. Fellers. *Polymer engineering and science,* 1984, **24**, 1327-1336.
15 Z. H. Yuan and B. D. Favis, *AIChE Journal* 2005, **51**, 271-280.
16 I. Luzinov, C. Pagnoulle and R. Jerome. *Polymer*, 2000, **41**, 7099-7109.
17 S. Ravati and B. D. Favis, *Polymer*, 2013, **54**, 3271-3281.
18 S. Ravati and B. D. Favis, *Polymer*, 2013, **54**, 6739-6751.
19 S. Ravati and B. D. Favis, *Polymer*, 2010, **51**, 3669-3684.
20 H. Gramespacher and J. Meissner, *Journal of Rheology*, 1992, **36**, 1127-1141.
21 P. H. P. Macaubas and N. R. Demarquette, *Polymer*, 2001, **42**, 2543-2554.
22 S. A. Saltikov, Proceedings of the second international congress for stereology, Springer-Verlag, New York, 1967, pp. 163-173.
23 M. Fialkowski, A. Bitner and B. A. Grzybowski, *Nature Material*, 2005, **4**, 93-97.
24 L. A. Utracki, Polymer alloys and blends. New York: Hanser; 1990.
25 N. Virgilio, P. Desjardins, G. L. Esperance and B. D. Favis, *Macromolecules*, 2009, **42**, 7518-7529.
26 V. Everaert, L. Aerts and G. Groeninckx, *Polymer*, 1999, **40**, 6627-6644.
27 T. Vacková, M. Slouf, M. Nevoralová and L. Kaprálková, *European Polymer Journal*, 2012, **48**, 2031-2039.
28 V. Everaert, G. Groeninckx and L. Aerts, *Polymer*, 2000, **41**, 1409-1428.
29 G. I. Taylor, The viscosity of a fluid containing small drops of another fluid. Proc. R. Soc. A 1932, 138, p. 41-48.
30 N. Virgilio, C. M. Aurele and B. D. Favis, *Macromolecules*, 2009, **42**, 3405-3416.
31 S. Horiuchi, N. Matchariyakul, K. Yase and T. Takeshi Kitano, *Macromolecules*, 1997, **30**, 3664-3670.
32 A. Pyun, J. R. Bell, K. H. Won, B. M. Weon, S. K. Seol, J. H. Je and C. W. Macosko, *Macromolecules*, 2007, **40**, 2029-2035.
33 T. S. Omonov, C. Harrats, G. Groeninckx and P. Moldenaers, *Polymer*, 2007, **48**, 5289-5302.
34 Z. Yuan and B. D. Favis, *J. Polym. Sci., B: Polym. Phys*, 2006, **44**, 711-721.
35 J. A. Galloway, H. K. Jeon, J. R. Bell and C. W. Macosko, *Polymer*, 2005, **46**, 183-191.
36 P. Sarazin and B. D. Favis, *Biomacromolecules*, 2003, **4**, 1669-1679.
37 P. Sarazin, X. Roy and B. D. Favis, *Biomaterials*, 2004, **25**, 5965–5978.
38 H, Veenstra, J. Van Dam and A. Posthuma de Boer, *Polymer*, 2000, **41**, 3037-3045.

Graphic abstract

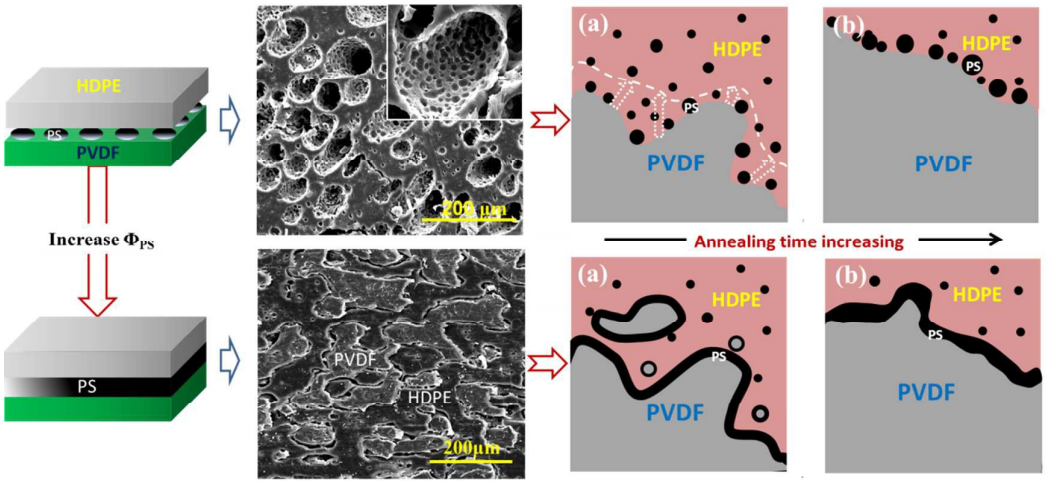

Highlights

A hierarchical tri-continuous structure is formed and controlled in PVDF/PS/HDPE ternary blends.

A very high level of PS continuity of about 80% in PVDF/PS/HDPE ternary blends is achieved only with a PS volume composition as low as 11vol %.

The evolution of phase morphology for PVDF/PS/HDPE ternary blends is well studied and discussed via melt annealing test.